



The Study of Chemical, Mechanical, Thermal, and Morphological Properties of Poly Lactic Acid-nano Hydroxyapatite Composite Scaffold

**Md Ruhul Amin Foisal^{1,2}, Ajoy Kumer^{2*}, Umma Taslima Nasrin¹,
Mohammad Ismail¹ and Mohammad Saiful Alam¹**

¹*Department of Applied Chemistry and Chemical Engineering, Noakhali Science and Technology University, Sonapur, Noakhali-3802, Bangladesh.*

²*Department of Chemistry, Bangladesh University of Engineering and Technology, Dhaka-1000, Bangladesh.*

Authors' contributions

This work was carried out in collaboration between all authors. Authors MRAF and MSA designed the study and wrote the protocol of the study. Authors MRAF and AK wrote the first draft of the manuscript. Authors MRAF, AK and UTN managed the chemical analysis, data analysis, instrumental analysis and mechanical analysis of the study. Authors MRAF, AK and MI managed the analyses, literature searches and performed the statistical analysis of the study. All authors read and approved the final manuscript.

Article Information

DOI: 10.9734/CSJI/2018/41184

Editor(s):

(1) Akmal S. Gaballa, Professor, Faculty of Specific Education, Zagazig University, Zagazig, Egypt.

Reviewers:

(1) Ioana Stanciu, University of Bucharest, Romania.

(2) Rafal Anyszka, Institute of Polymer and Dye Technology of Lodz University of Technology, Poland.

Complete Peer review History: <http://www.sciencedomain.org/review-history/24712>

Original Research Article

Received 26th February 2018

Accepted 8th May 2018

Published 21st May 2018

ABSTRACT

Hydroxyapatite (HAp) ceramics have been recognized as substitute material in bone due to their chemical and biological similarity to human bone tissue. Nano HAp powders were synthesized by wet precipitation technique using aqueous suspension of 0.5 M calcium hydroxide [Ca(OH)₂] with 0.3 M orthophosphoric acid [H₃PO₄] adding drop-wise and vigorously stirred to control the crystal size at nanoscale room temperature and pH 10.0 were maintained to obtain a high purity of HAp. The HAp has been characterized and confirmed its nano crystal formation by X-ray diffraction (XRD). Then HAp has been pushed through polylactic acid (PLA) to make the composite scaffold

*Corresponding author: E-mail: kumarajoy.cu@gmail.com;

blocks. Nano HAp-PLA composite scaffold blocks were produced by freeze drying. Different loading concentrations of nano-hydroxyapatite (nHAp) particles with the polylactic acid (PLA) fabricated scaffold blocks was investigated on their mechanical, thermal and morphological properties. The chemical and thermal properties of scaffold blocks were investigated by X-ray diffraction (XRD), the simultaneous thermo-gravimetric analyzer (TGA), the differential thermal analyzer (DTA) and thermos-mechanical analyzer (TMA). Crystallographic characterization was done by X-Ray diffraction and morphological characterization by scanning electron microscope. From the mechanical, thermal, chemical, and morphological analysis, it can estimate that the scaffold blocks possess microporous structure with 60% porosity having low moisture content 3% maximum, uniform nHAp distribution through scaffold block and 15% HAp contained scaffold block possess maximum load holding ability.

Keywords: Hap; scaffold; x-ray diffraction analysis; thermo gravimetric analysis; differential thermal analysis; and thermo mechanical analysis.

1. INTRODUCTION

The main object of tissue engineering is to develop the replacement tissues to repair damaged organs. Among the applications of tissue engineering to repair damaged organs such as livers, hearts, and bones, bone repair by tissue engineering may be one of the first major applications to succeed. The design of bioresorbable scaffolding materials and the manufacturing technology of porous scaffolds are at the bone tissue engineering approaches [1]. The scaffolds serve as a three-dimensional template for initial cell attachment and subsequent tissue regeneration [2]. Fabrication of porous scaffolds from advanced biomaterials for healing bone defects represents a new approach for tissue engineering that aims at the enlargement of biological substitutes that renovated maintain or improve tissue function [3]. Hydroxyapatite (HAp) ceramics is the common material used as the replacement material in bone tissue. It is biocompatible and bioactive material that can be used to restore damaged human calcified tissue. HAp cannot be implanted directly as a healing supplement in calcified tissue. HAp, when blended with polylactic acid (PLA), not only improved the bending strength of the composite but also had an active role in new bone formation. In a typical tissue engineering approach, to control tissue formation in three dimensions (3D), a considerable porous scaffold is critical [4]. In addition to defining the 3D geometry for the tissue to be engineered, the scaffold provides the microenvironment (synthetic temporary extracellular matrix) for regenerative cells, supporting cell attachment, proliferation, differentiation, and neo tissue genesis [4-5]. Different calcium phosphate phases have been used for the fabrication of such printed ceramics HAp tricalcium phosphate

and HAp/tricalcium phosphate, tricalcium phosphate/calcium pyrophosphate and tetracalcium phosphate, as well as granules consisting of b-tricalcium phosphate and bioactive glass. Besides sintering, established a polymer infiltration process to improve the mechanical properties of the printed structures described a low-temperature 3D printing process, in which samples consisting of the calcium phosphate phase brushite were obtained by initiation of a cement setting reaction, which can be further transformed into monetite by hydrothermal conversion [6]. The low-temperature phase brushite and monetite, which cannot be generated by sintering, are known for their faster restoration compared to HAp, due to their higher solubility at the physiological condition. Therefore, the chemical compositions, physical structure, and biologically functional moieties are all important attributes to biomaterials for tissue engineering. HAp is the developing bio-ceramic, which is composed primarily of calcium and phosphorous with hydroxide ions that are eliminated at elevated temperatures [7]. HAp and other related calcium phosphate materials widely used in various biomedical applications due to its excellent biocompatibility and bone bonding ability and its close similarities with the inorganic mineral phase of human bone tissue [1]. Synthetic HAp is similar to naturally occurring HAp in contrast to crystallographic and chemical studies. The ratio of Ca/P is to be 1.667 to promote intimate bone growth onto femoral implant [8]. The quality of a scaffold is closely dependent on the overall attributes and characteristics of the synthesized powders. Such attributes include phase composition, purity, crystallinity, particle size, particle-size distribution, specific surface area, density and particle morphology [9]. These important factors determine the resulting success

of the HAp/PLA scaffold onto orthopedic implants [10]. Use of calcium phosphate polymer composites creates a highly biocompatible product by increasing cell-material interactions compared to the polymer alone [11]. Furthermore, the sustained release of calcium and phosphate from those composites, where the two ions serve as substrates in the remodeling reactions of mineralized tissues is an added benefit [2].

Biodegradable polyesters, such as poly (lactic acid) (PLA), poly (glycolic acid) (PGA) and their copolymers (PLGA), have been widely used for the preparation of tissue engineering scaffolds due to their good biodegradability and processing properties [12]. However, they are over flexible and of insufficient strength to meet the mechanical demands of bone replacement, nor do they present a favorable surface for cell attachment and proliferation because of their lack of specific cell-recognizable signals [13].

Due to the extensive use of PLAs in the biomedical field[5], their composites with HAp constitute the most common materials in the literature about biodegradable hard tissue implants. HAp, when blended with PLA, not only improved the bending strength of the composite but also had an active role in new bone formation [14].

The HAp surface was found to be highly reactive and led to favorable attachment to tissue and bioactivity in bone repair [15-16]. In this work, the primary purpose was to increase the reactivity of HAp attachment to bone tissue by increasing HAp's surface area which was done by synthesis of nano HAp crystal. And the secondary purpose was to find a suitable composition percentage of nano HAp/PLA composite that can possess similarity with bone tissue.

2. METHODOLOGY

2.1 Materials

Calcium Hydroxide (Sigma-Aldrich, Reagent Plus, $\geq 97\%$), Phosphoric Acid (85% solution, Sigma-Aldrich), and Ammonium Hydroxide (NH_4OH) (Sigma-Aldrich) were purchased from the chemical companies and used without purification.

2.2 Preparation of Nano HAp Powders

Calcium Hydroxide (74.09 g/mol, density: 3.16 gm/cm^3) was dried under vacuum at 75°C before

synthesis of nHAp. The 50 ml of 0.3M orthophosphoric acid [H_3PO_4] (85% solution, 97.995 g/mol, density: 1.685 g/ml) was added with 50 ml aqueous suspension of 0.5 M calcium hydroxide [$\text{Ca}(\text{OH})_2$] at room temperature and the pH (10.5) was maintained by adding dropwise 1 M ammonium hydroxide [$\text{NH}_4(\text{OH})$] solution(28-30%)to obtain nanoHAp powders via precipitation method [8,17]. The suspension was well stirred (1000 rpm) using magnetic stirrer for 2 hours and aged for overnight at room temperature (Fig. 1). In the second day, the suspension was heated at 150°C for 2 hours and stirred at 1000 rpm then cooled at room temperature. After that, the suspension is sonicated at ultrasonication bath with 30 minutes period for 6 times and finally high-speed stirring at 1500 rpm for 6 hours, and then aging for 24.0 hours. On the fourth day, the precipitates were subjected to vacuum filtrating using Buchner funnel, repeatedly washed with deionized water and filtered again. The precipitates were dried at 80°C for 48 hours. Dried lumps of powders were ground by clean pestles and mortars.

2.3 Preparation the Different % of Nano HAP/PLA Composite

The required quantity (Table-1) of nHAp powder was dispersed in 1,4-Dioxane (88.11 g/mol, density 1.003 g/cm^3); by sonication, then following the table required an amount of Poly Lactic Acid (density 1.29 g/cm^3) was added to the mixtures and stirred at 50°C until complete dissolution. Four solutions with different content in nHAp were prepared, 5%, 10%, 15%, 20% particle by weight with regard to PLA. The nHAp/PLA solution was poured aluminium foil and frozen in 0°C for 24 hours. Then the scaffolds were placed in freeze dryer in order to remove the dioxane. After extraction of dioxane, the scaffold was dried in atmospheric temperature and then cut into cubes (1 cm x 1 cm x 1 cm). These samples were then again dried at 40°C in a vacuum dryer and stored in desiccators.

2.4 Determination of Porosity

The estimated density and porosity of the matrix were obtained as follows. The volume of the matrix is calculated using suspended weight. And the mass of the matrix was measured with an analytical balance. The density was calculated from the volume and mass. The porosity, ϵ , was calculated from the measured overall density D_m of the matrix and the skeletal density D_s . For a

composite scaffold, the skeletal density was determined using the densities of the polymer and nHAp powder. The porosity was given by,

$$\varepsilon = \frac{D_s - D_m}{D_s} \quad (1)$$

Where,

D_s was calculated from the following formula:

$$D_s = \frac{1}{\frac{1-X_h}{D_p} + \frac{X_h}{D_h}} \quad (2)$$

Where D_h is the density of the nHAp powder with a value of 3.16 gm/cm^3 and X_h is the percentage of nHAp in the composite scaffold while D_p is the density of the polymer.

2.5 X-ray Diffraction Analysis

XRD analysis was carried out with a powder diffract -meter where the sliced sample was directly put into the sample holder and then experiment was carried out. Gobel Mirror was the source of X-ray. The filter was used to removing $\text{CuK}\beta$ and Soller slit to pass the parallel ray. The peaks obtained were used to determine the exact crystal structure of the nHAp. XRD studies have

been carried out by D8 Advance, Bruker AXS, Germany. The exact crystalline structure of the samples confirmed by XRD revealed the formation of the calcium-Hydroxyapatite phase and yielded reflections.

2.6 Scanning Electron Microscopy Analysis

Image analysis was carried out using a Scanning Electron Microscope (SEM) (model: JSM-6490LA) for observing surface morphology, particle size, particle distribution, porosity, and pore size. It is a High-performance, SEM with an embedded energy dispersive X-ray analyzer (EDS) with allows for seamless observation and EDS analysis.

2.7 Thermogravimetric Analysis

TGA/DTA and DTG studies have been done by TG/DTA 6300, SII NanoTechnology Japan, system controlled by an EXSTAR 6300 controller. TGA and DTA studies have been carried out on freeze-dried nHAp/PLA composite scaffold sample in different weight percentage. Experiments have been performed using simultaneous TGA-DTA analysis by heating the sample at 20° C/min in the temperature range 30° C and 60° C in nitrogen atmosphere.

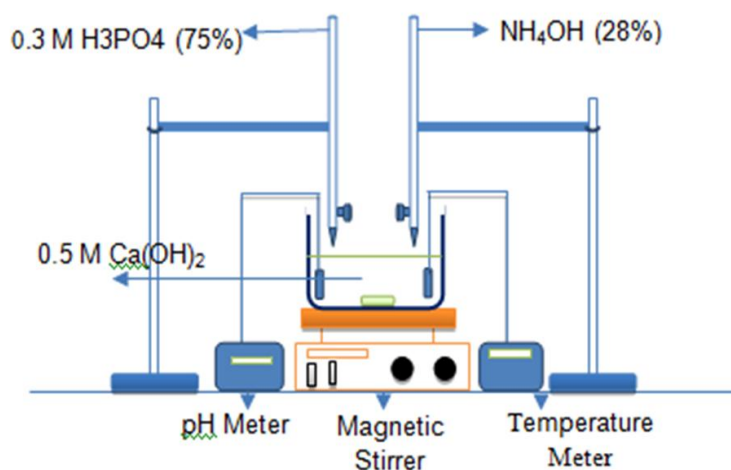


Fig. 1. Schematic drawing of apparatus for nanoHAp powders synthesis

Table 1. Weighing of the composition for scaffold preparation

Sample name	nHAp (gm)	PLA (gm)	1,4-Dioxane (ml)
5%nHAp/PLA	0.2002	4.048	15
10%nHAp/PLA	0.4008	4.043	15
15%nHAp/PLA	0.6022	4.019	15
20%nHAp/PLA	0.8019	4.032	15

2.8 Thermo-mechanical Analysis

TMA studies have been done by TMA/SS 6300, SII Nano Technology, Japan, system controlled by an EXSTAR controller. TMA studies have been carried out on the nHAP/PLA composite scaffold in different percentage. Experiments have been performed using simultaneous TMA analysis by heating the sample at 50C/min in the temperature range 30°C and 100° C in nitrogen atmosphere.

3. RESULTS AND DISCUSSION

3.1 Porosity Analysis

nHAP/PLA composite scaffolds with high porosity have been fabricated using freeze drying. One solvent systems were used to obtain composite scaffolds with pore structures, is a mono-solvent system of pure 1, 4-dioxane. The density and porosity of scaffolds are found 60%, 59%, 58% and 57% for 5%, 10%, 15% and 20% nHAP/PLA composite Scaffold respectively. Incorporation of nano-sized HAP only decreased the porosity slightly. Regardless of detailed morphology and composition, all scaffolds have a porosity of at least 57%, which was considered to be beneficial for a cell in growth and survival. The solvent system did not have much effect on the density but its amount controls the porosity.

3.2 X-RD Analysis

The sample nanoHAP exhibits almost same diffraction pattern with the characteristic peaks of standard HAP. The peak analysis of the XRD pattern shows 14.9 nm crystal size and the exact crystalline structure of the sample with $Ca/P = 1.65$.

3.3 Comparison of XRD Pattern of 5%, 10%, 15%, 20% nHAP/PLA Composite Scaffold Matrix with Standard Hap

The analysis of scaffold with XRD shows the growing intensity of the nHAP with the increasing of the weight percentage. XRD analysis of the nHAP/PLA composite scaffold shows that with the increasing percentage of HAP content the nHAP characteristic peaks intensity increases as the nHAP content in increases in the scaffold sample.

3.4 Effect of HAp Content on the Structure and Mechanical Properties of Scaffold

3.4.1. Scanning electron microscopic analysis

The effects of nanoHAp percentage present on the structure of nanoHAP/PLA composite have been investigated. It was clear that there was no large-scale variation among the variables of HAp percentage. The first sample comprising 5% HAp in PLA matrix exhibit relatively large crystal size and pore size of 35µm Fig.3 whereas the sample with 20% HAp in PLA matrix revealed a smaller pore size of a 30µm Fig. 3. From this analysis, it was clearly identifiable that the porous nature of these composites are regular and the pore size also regular.

3.4.2 Determination of weight loss by thermogravimetric analysis(TGA)

TGA and DTGA show that all the sample exhibited two distinct weight loss stages at 40⁰C-110⁰C (maximum 5.2% and minimum 2%) the weakly bonded water. 300⁰C-450⁰C (decomposition of the main chain of PLA). The major weight loss is observed in the 300⁰C-450⁰C region for the entire sample. That is corresponding to the structural decomposition of PLA. First order derivative of TGA curves reveals the temperature at which the maximum decrease of mass occurs. The temperature at the maximum loss rate is 378.0⁰C, 378.1⁰C, 378.10C and 378.7⁰C for 5%, 10%, 15%, and 20% HAP content in PLA respectively. So it is clear that the HAp percent is not affecting the PLA breakdown.

3.5 Comparative Thermo-gram of 5%, 10%, 15%, 20% nHAP/PLA Composite Scaffold

From the comparison, it shows a clear result of uniform sample composite. According to residue analysis, it was found that with increasing percentage of the HAp content the residue percentage of the sample increases simultaneously. The differential thermo gravimetric analysis (DTG) shows the decomposition temperature of PLA is same for the entire composite. So it can summarize the decomposition of PLA does not affect the nanoHAp content.

Table 2. Calculation of the porosity nHAp/PLA composite scaffold

	Sample dry weight(gm)	The suspended weight of water (gm)	Sample volume (cm ³)	The density of the matrix should be (gm)	The actual density of the matrix (gm)	Porosity	Average Porosity
5% HAp/PLA	0.0891	0.1733	0.1733	1.288954	0.514137	0.601121	0.605 60%
	0.0827	0.1616	0.1616	1.288954	0.511757	0.602967	
	0.0755	0.1502	0.1502	1.288954	0.502663	0.610023	
10% HAp/PLA	0.0697	0.1275	0.1275	1.330414	0.546667	0.5891	0.594 59%
	0.0632	0.1173	0.1173	1.330414	0.538789	0.595021	
	0.0637]	0.1190	0.119	1.330414	0.535294	0.597649	
15% HAp/PLA	0.09	0.1584	0.1584	1.37463	0.568182	0.586666	0.582 58%
	0.0892	0.1538	0.1538	1.37463	0.579974	0.578087	
	0.0963	0.1678	0.1678	1.37463	0.573897	0.582508	
20% HAp/PLA	0.0797	0.1309	0.1309	1.421886	0.608862	0.571793	0.575 57%
	0.0618	0.1019	0.1019	1.421886	0.606477	0.57347	
	0.0774	0.1292	0.1292	1.421886	0.599071	0.578679	

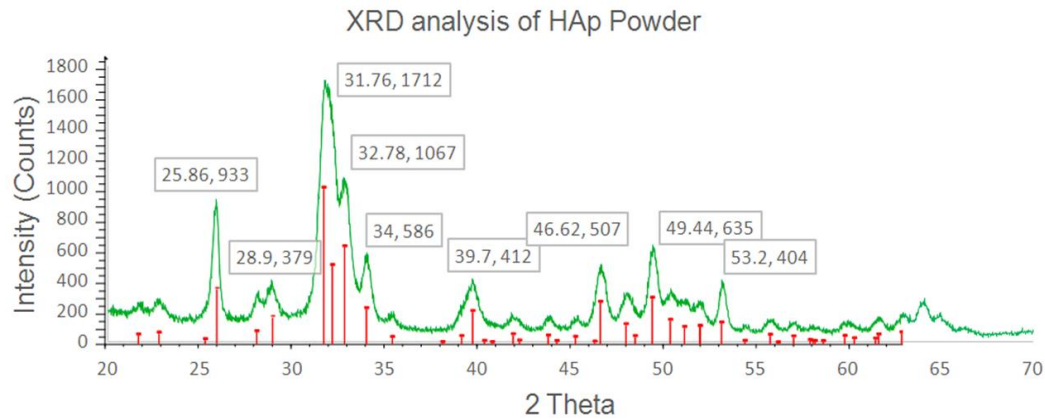


Fig. 2. XRD pattern of hydroxyapatite particle with comparing the standard sample of Hap

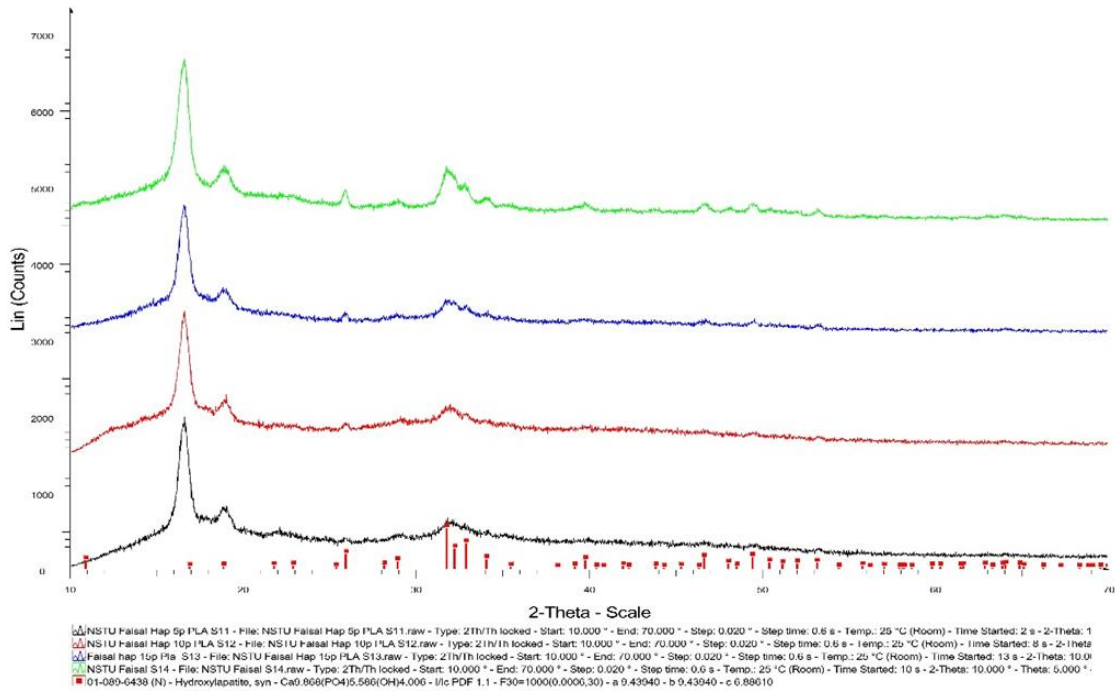


Fig. 3. Comparison of XRD pattern of 5%, 10%, 15%, 20% nHAp/PLA Composite Scaffold matrix with standard HAp

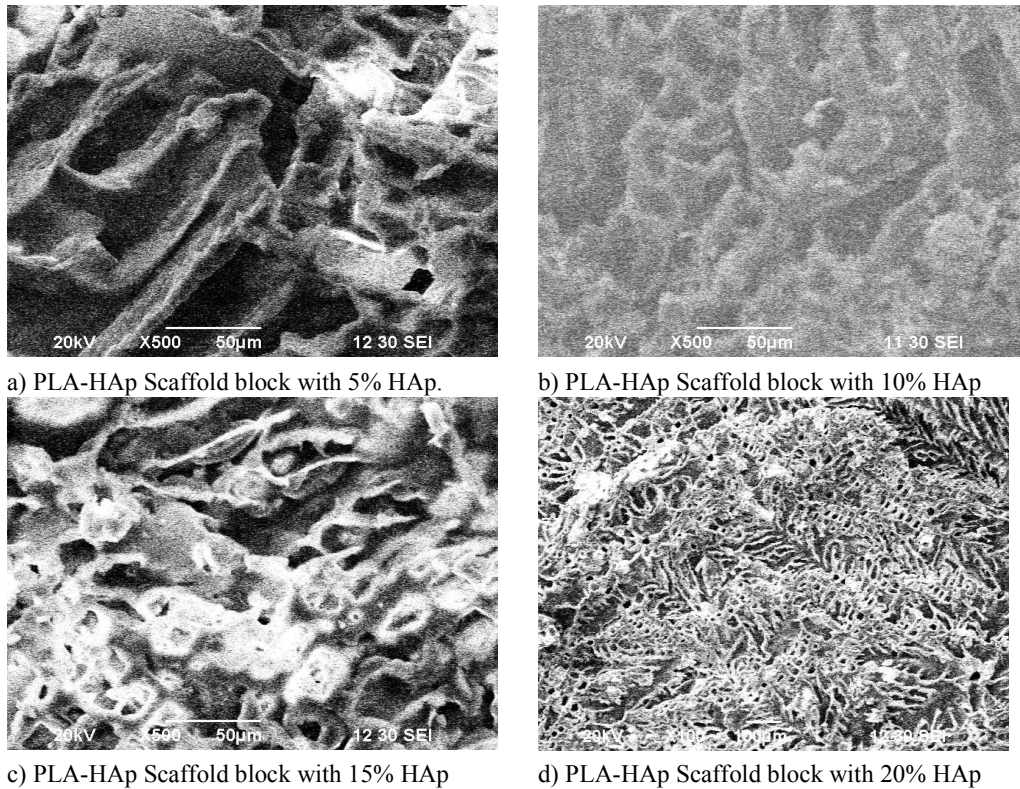


Fig. 4. SEM microstructure of composite scaffold block

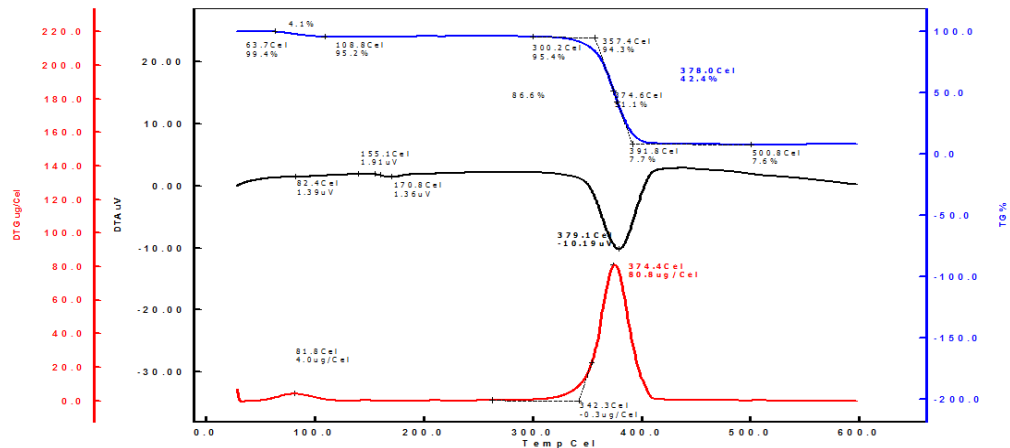


Fig. 5. Thermogram of 5% nHAp/PLA composite scaffold

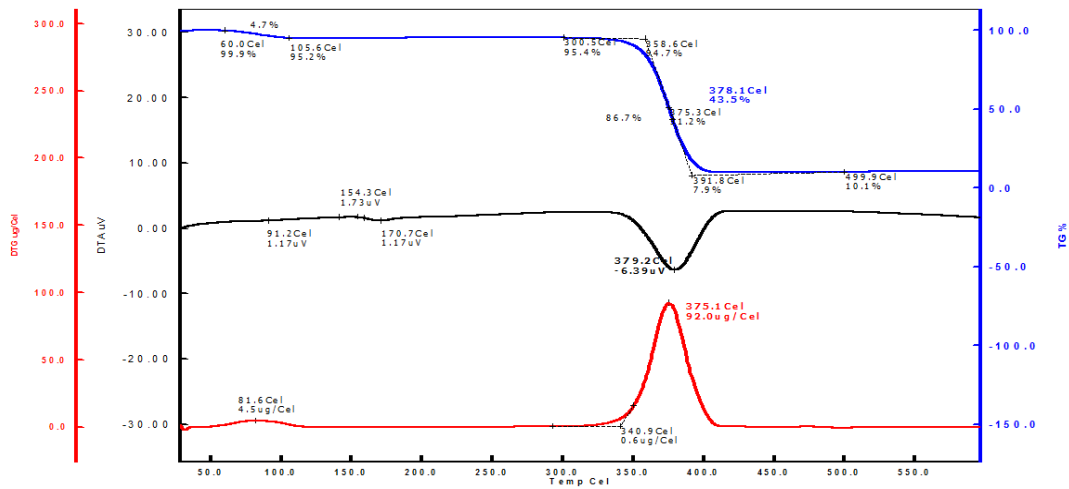


Fig. 6. Thermogram of 10% nHAp/PLA composite scaffold

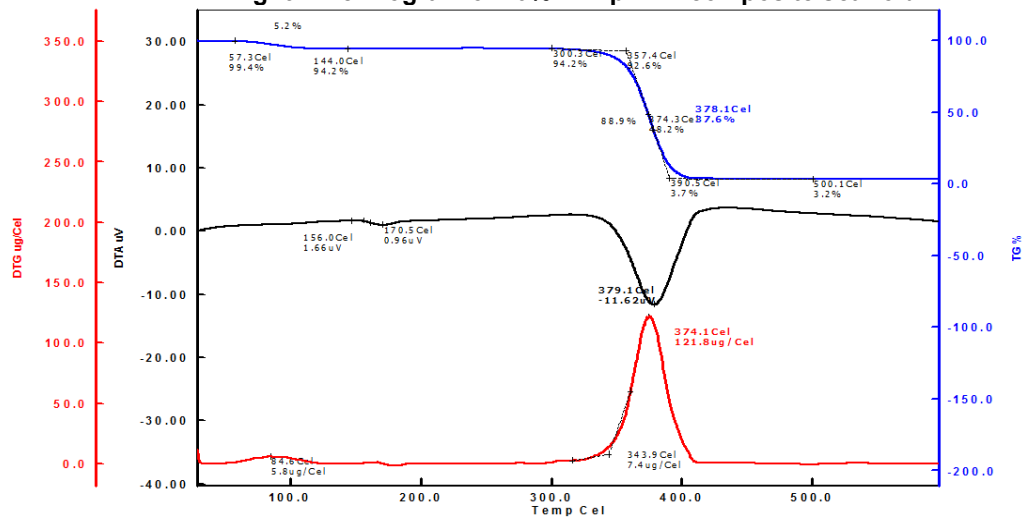


Fig. 7. Thermogram of 15% nHAp/PLA composite scaffold

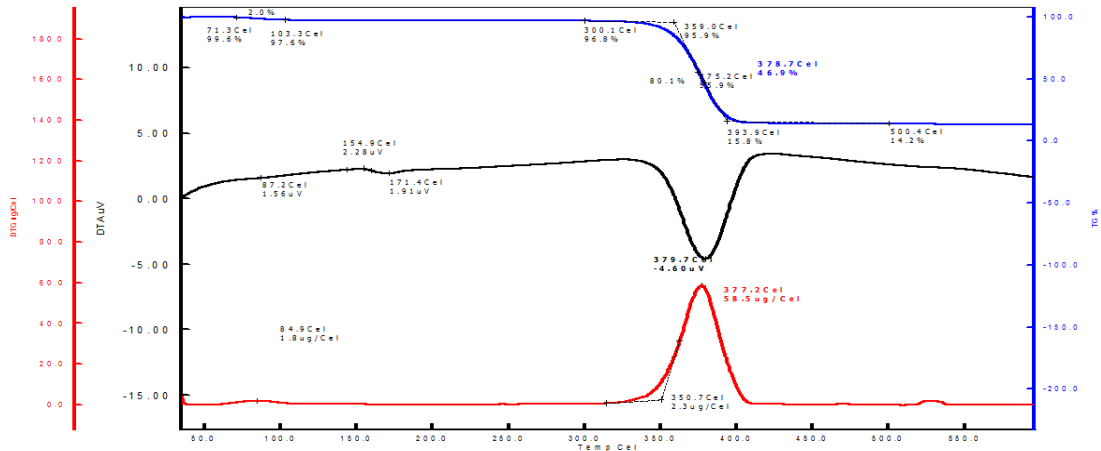


Fig. 8. Thermogram of 20% nHAp/PLA composite scaffold

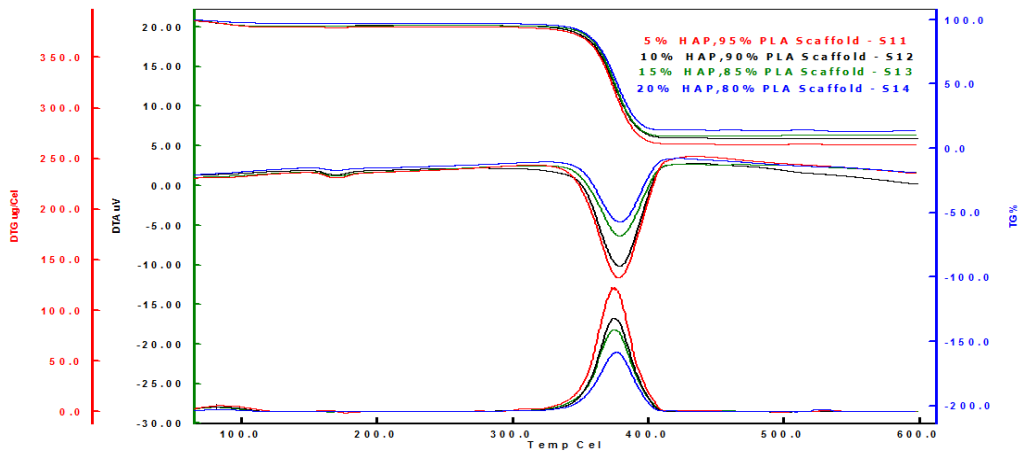


Fig. 9. Comparative thermo-gram of 5%, 10%, 15%, 20% nHAp/PLA composite scaffold

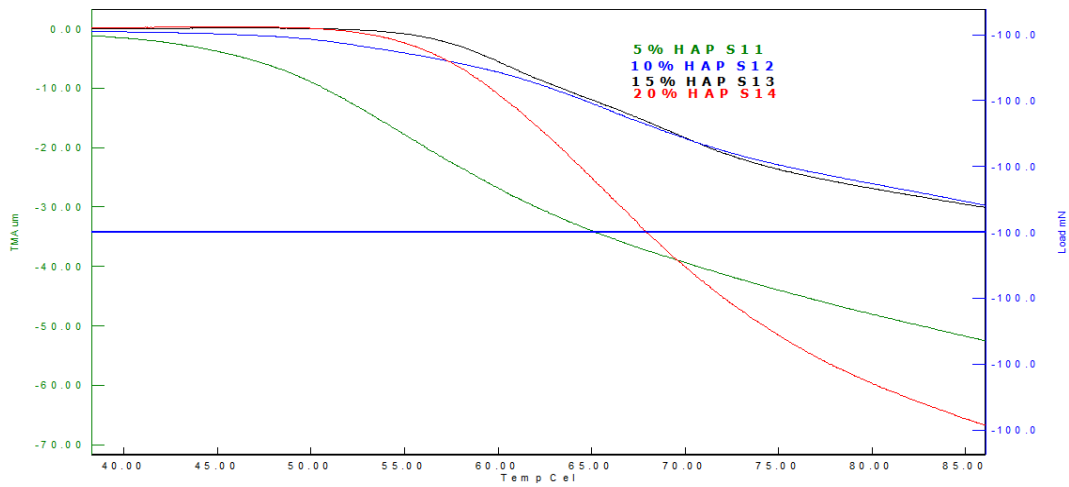


Fig. 10. Comparison of thermo mechanical thermogram of 5%, 10%, 15% and 20% nHAp/PLA composite scaffold

3.6 Determination of different loading by (thermo mechanical analysis) TMA

TMA shows the load holding temperature 46.8⁰C, 49.8⁰C, 55.57⁰C and 55.08⁰C respective to 5%, 10%, 15% and 20% nHAp/PLA composite scaffold. As from the DTGA result, the change in HAp percentage does not influence the characteristics of PLA. So it can be summarized the change in the mechanical load holding varies only due to the change in the percentage of HAp. And the optimum HAp content found in the 15% HAp composite sample, which possesses the most similar properties as like bone.

4. CONCLUSION

The powerful technique for fabricating biocompatible and biodegradable nHAp/PLA composite scaffold is effective for development of the method. So that to mimic mineralized hard tissues for bone regeneration purpose by matrix mediated in situ syntheses of nHAp/PLA composite scaffold was followed by the freeze-thawing process. Various techniques, including SEM, XRD, TMA, and TGA were performed to characterize the resulting nHAp/PLA composite scaffold. Morphological investigation showed that the HAp particles exhibit micro-porous morphology, which provides enlarge interfaces being a prerequisite for physiological and biological responses and remodeling to integrate with the surrounding native tissue.

ACKNOWLEDGEMENTS

The author gratefully acknowledges to Dr. Md. Abdul Gafur, Senior Scientific Officer, PP & PDC, BCSIR, and Md. Rakibul Islam, Engineer, PP & PDC, BCSIR.

COMPETING INTERESTS

Authors have declared that no competing interests exist.

REFERENCES

1. Katy Rutledge QC, Marina Pryzhkova, Greg M. Harris, Ehsan Jabbarzadeh. Enhanced differentiation of human embryonic stem cells on extracellular matrix-containing osteomimetic scaffolds for bone tissue engineering. *Tissue Engineering Part C: Methods*. 2014; 20(11):865-874.
2. Skrtic D AJ, Eanes ED. Amorphous calcium phosphate-based bioactive polymeric composites for mineralized tissue regeneration. *Journal of Research of the National Institute of Standards and Technology*. 2003;108:167-182.
3. Stevens MM. Biomaterials for bone tissue engineering. *Biomaterials*. 2008;11(5):18-25.
4. Aurelio Salerno DG, Maria Iannone, Stefania Zeppetelli, Paolo A. Netti. Effect of micro- and macroporosity of bone tissue three-dimensional-poly(ϵ -Caprolactone) scaffold on human mesenchymal stem cells invasion, proliferation, and differentiation *in vitro*. *Tissue Engineering Part A*. 2010;16(10):2661-2673.
5. Adele Boskey NPC. FT-IR imaging of native and tissue engineered bone and cartilage. *Biomaterials*. 2007;28(15):2465-2478.
6. Ye Xu DW, Lan Yang, Honggao Tang. Hydrothermal conversion of coral into hydroxyapatite. *Materials Characterization*. 2001;47(2):83-87.
7. Mythili Prakasam JL, Kristine Salma-Ancane, Dagnija Loca, Alain Largeteau, Liga Berzina-Cimdina. Fabrication, properties and applications of dense hydroxyapatite: A review. *Journal of Functional Biomaterials*. 2015;6(4):1099-1140.
8. Manuel CM, FM, Monteiro FJ. Synthesis of hydroxyapatite and tri calcium phosphate nanoparticles. *Preliminary Studies*. *Key Eng Mater*. 2003;555-58.
9. Naruporn Monmaturapoj AS, Prasert Chalermkarnon, Suthawan Buchatip, Atitsa Petchsuk, Warobon Noppakunmongkolcha, Katanchalee Mai-Ngam. Properties of poly(lactic acid)/hydroxyapatite composite through the use of epoxy functional compatibilizers for biomedical application. *Journal of Biomaterials Applications*. 2017;0(0):1-16.
10. Aurelio Salerno MFG, Julio San Román del Barrio. Concepción Domingo Pascual, macroporous and nanometre scale fibrous PLA and PLA–HA composite scaffolds fabricated by a bio safe strategy *Royal Society of Chemistry: Advanced*. 2014; 4(106):61491-61502.
11. Rizzi SC, et al. Biodegradable polymer/hydroxyapatite composites: Surface analysis and initial attachment of human osteoblasts. *Journal of*

- Biomedical Materials and Review. 2001;55:575-486.
12. Weraporn Pivsa-Arta* AC, Sommai Pivsa-Arta, Hideki Yamanec, Hitomi Oharac. Preparation of Polymer blends between poly(lactic acid) and poly(butylene adipate-co-terephthalate) and biodegradable polymers as compatibilizers. Energy Procedia. 2013.34:549-554.
 13. Mohammad Ismail MRAF, Ajoy Kumer, Omma Taslima Nasrin, Muhammad Zakarul Islam. Physical and mechanical characterization of jute fiber reinforced unsaturated polyester resin (UPR) composites. Chemical Science International Journal. 2018. 22(2):1-14.
 14. Furukawa TMY, Yasunaga T, Shikinami Y, Okuno M, Nakamura T. Biodegradation behavior of ultra-high-strength hydroxyapatite/poly (L-lactide) composite rods for internal fixation of bone fractures. Biomaterials. 2000;21(9):889-898.
 15. Ducheyne PQQ. Bioactive ceramics: The effect of surface reactivity on bone formation and bone cell function. Biomaterials. 1999;20:2287-2303.
 16. Filippo Rossi MS, Giuseppe Perale. Polymeric scaffolds as stem cell carriers in bone repair. Journal of Tissue Engineering and Regenerative Medicine. 2015;9(10): 1093-1119.
 17. Xiang-Fang Peng HY, Xin Jing, PengYu, Jin-Ping Qu, Bin-Yi Chen. Preparation of highly porous interconnected poly(lactic acid) scaffolds based on a novel dynamic elongational flow procedure. Materials and Design. 2016;101:285-293.

© 2018 Foissal et al.; This is an Open Access article distributed under the terms of the Creative Commons Attribution License (<http://creativecommons.org/licenses/by/4.0>), which permits unrestricted use, distribution, and reproduction in any medium, provided the original work is properly cited.

Peer-review history:

*The peer review history for this paper can be accessed here:
<http://www.sciencedomain.org/review-history/24712>*